

Formation of rogue waves from the locally perturbed condensate

A. A. Gelash^{1,2*}

¹*Novosibirsk State University, Novosibirsk, 630090, Russia and*

²*Institute of Thermophysics, SB RAS, Novosibirsk, 630090, Russia*

(Dated: May 9, 2019)

The one-dimensional focusing nonlinear Schrödinger equation (NLSE) on the unstable condensate background is one of the most important models of rogue waves formation. Complete integrability of the NLSE via Inverse Scattering Transform allows decomposition of an initial condition into elementary nonlinear modes: breathers and continuous spectrum waves. The small localized condensate perturbations (SLCP) that grow as a result of modulation instability (MI) are of fundamental interest in nonlinear physics for many years. Here we demonstrate, that the so called superregular NLSE breathers play the key role in the dynamics of a wide class of SLCP. At the nonlinear stage of MI development collisions of superregular breathers lead to the formation of rogue waves. We present scenarios of rogue waves formation for randomly distributed superregular breathers as well as for artificially prepared initial conditions. For the latter case we give analytical description based on the found exact expressions for space-phase shifts, that breathers acquire after collisions with each other. Finally, the presence of superregular breathers in arbitrary-type condensate perturbations is demonstrated by solving Zakharov-Shabat eigenvalue problem with high numerical accuracy.

A. Introduction

The formation of extreme amplitude waves is one of the most remarkable phenomenon in physics of wave processes. In the linear case these events may appear only as a result of simple wave interference, while the interactions of nonlinear waves exhibit wide range of non-trivial mechanisms such as modulation instability (MI) development or nonlinear wave focusing [1, 2]. The so-called *rogue (freak)* waves are of special attention as they suddenly appear from relatively weak perturbations of a calm background. This unusual phenomenon is observed experimentally in different nonlinear media such as optical fiber with Kerr nonlinearity, Bose-Einstein condensate and surface of a fluid [3–5].

The one-dimensional focusing nonlinear Schrödinger equation (NLSE):

$$i\psi_t - \frac{1}{2}\psi_{xx} - (|\psi|^2 - A^2)\psi = 0, \quad (1)$$

is one of the most fundamental mathematical model describing weakly nonlinear wave propagation accompanied by the formation of rogue waves. Here $\psi(t, x)$ is the complex valued wavefield, t and x are the time and space coordinates and the meaning of the constant A is discussed below.

In the early 70's V.E. Zakharov and A.B. Shabat found that the NLSE with infinite line vanishing boundary conditions (BC) can be completely integrated using a very powerful technique – the Inverse Scattering Transform (IST) [6]. In 1977 E.A. Kuznetsov [7] and later Y.C. Ma, T. Kawata and H. Inoue [8, 9] studied the case of the NLSE on the so-called *condensate* background – simple quasi-monochromatic plane wave solution of the NLSE.

In this work we write the condensate solution of the equation (1) as $\psi_0(t, x) = A$, where A is the background amplitude, that we assume to be real without loss of generality (the limit of vanishing BC corresponds to the case $A = 0$). The condensate is unstable with respect to long-wave perturbations (MI), with the following growth rate:

$$\Gamma(k) = k\sqrt{A^2 - k^2/4}, \quad (2)$$

where k is the perturbation wave number. It means, that in the region: $0 < k < 2$, the amplitude of such perturbations grows $\sim e^{\Gamma t}$ at the initial (linear) stage. The nonlinear stage of MI development may lead to the formation of rogue waves (see, for instance [2]).

The NLSE on the condensate background has a large family of exact solutions such as Peregrine [10], Kuznetsov-Ma [7, 8] and Akhmediev [11] breathers. Moreover, the IST links the initial wave field with so called *scattering data*, which play the role of non-interacting nonlinear modes – similar to Fourier harmonics in the linear wave theory. The evolution of scattering data is trivial that allows to find N -breather solution analytically and implicitly solve the general Cauchy problem via the integral Gelfand-Levitan-Marchenko equations (GLME). The scattering data are presented by discrete (breathers) and continuous (nonlinear dispersive waves) parts of the eigenvalue spectrum of Zakharov-Shabat auxiliary linear system (ZH system).

However, the nontrivial interactions of breathers and continuous spectrum waves with unstable condensate background and between each other makes the system evolution complicated and brings many fundamental questions. One of them is the long-time evolution of unstable small localised condensate perturbations (SLCP). In the mentioned paper [7], E.A. Kuznetsov suggested that the MI in this case is driven by unstable part of continuous spectrum waves and leads (at final stage) to a sort of local (i.e. at the area of initial perturbation) Fermi-Pasta-Ulam (FPU) recurrence to the unperturbed con-

*Electronic address: gelash@srd.nsu.ru

densate. In 2017 E.A. Kuznetsov presented a qualitative explanation, that such local recurrence can be explained by representation of the condensate background as a particular limiting case of a soliton lattice [12]. The other important results were recently obtained by G. Biondini et al. [13, 14]. They analytically describe the MI of continuous spectrum waves using asymptotic analysis of the GLME on the condensate background.

For a long time, the role of discrete spectrum solutions in the development of SLCP was attributed only to a particular class of Peregrine-type multi-breather rational solutions. They are known as the simplest analytical model of the rogue waves formation and also called *rational rogue waves* (see, for instance, the papers [15, 16]). In 2010 V.I. Shrira and V.V. Geogjaev broaden this approach to the wide subclass of Kuznetsov-Ma breathers [17]. The pure rational rogue wave scenario of MI development leads to the complete FPU recurrence, while the general scenario with Kuznetsov-Ma breathers demonstrates long time standing oscillations.

Recently V.E. Zakharov and A.A. Gelash found that the NLSE breathers may be hidden in SLCP at the moment of their pairwise collisions. Based on this observation they suggested new scenario of MI development which describes the formation of moving interacting breathers at the intermediate stage and local recurrence to the unperturbed condensate at large times [18, 19]. The experimental confirmation of these theoretical results was obtained simultaneously in optics and hydrodynamics by B. Kibler et al [20]. The later study of generalized NLSE and modified KdV models reveals the universal character of superregular breathers [21, 22]. However, the role of superregular breathers in the development of arbitrary-type (random) SLCP is unclear so far. In this paper we prove, that superregular breathers are contained in wide class of arbitrary-type initial conditions and demonstrate that they play the key role in the formation of rogue waves from the locally perturbed condensate.

B. Breather solutions of the NLSE

The eigenvalue problem for ZH system can be written in the following form:

$$\widehat{L}\Phi = \lambda\Phi, \quad \widehat{L} = \begin{pmatrix} 1 & 0 \\ 0 & -1 \end{pmatrix} \frac{\partial}{\partial x} - \begin{pmatrix} 0 & \psi \\ \psi^* & 0 \end{pmatrix}. \quad (3)$$

Here $\Phi(x, t, \lambda)$ is the matrix wave function (eigenfunction), while λ is the spectral parameter defined on the two-sheeted Riemann surface containing branchcut on the interval $[-A, A]$. The N -breather solution corresponds to N discrete eigenvalues λ_n on the right half of λ -plane, while continuous spectrum eigenvalues lies on the imaginary axis plus the branchcut.

In our previous works [18, 19] we use the so-called Joukowski transform of spectral parameter λ to simplify

theoretical analysis of N -breather solutions:

$$\lambda = \frac{A}{2} \left(\xi + \frac{1}{\xi} \right), \quad \xi = re^{i\alpha} = e^{z+i\alpha}. \quad (4)$$

In such variables the two-sheeted Riemann surface transforms into the one-sheeted ξ -plane. The line of branchcut $[-A, A]$ transforms into a circle of unit radius, while Riemann sheets become the outer and inner parts of the circle (see [19] for details).

In ξ variable the general one-breather solution of the NLSE (1) can be obtained in the following elegant form [19]:

$$\begin{aligned} \psi_1 &= Ae^{-i\theta_c} N_1 / \Delta_1, \quad (5) \\ N_1 &= \cosh z \cos 2\alpha \cosh 2u + \cosh 2z \cos \alpha \cos 2v \\ &\quad + i(\cosh z \sin 2\alpha \sinh 2u + \sinh 2z \cos \alpha \sin 2v), \\ \Delta_1 &= \cosh z \cosh 2u + \cos \alpha \cos 2v, \end{aligned}$$

where

$$\begin{aligned} u &= \varkappa(x - x_0) - \gamma t, & v &= \eta x - \omega t - \theta/2, \\ \varkappa &= A \sinh z \cos \alpha, & \gamma &= -A^2 \cosh 2z \sin 2\alpha/2, \\ \eta &= A \cosh z \sin \alpha, & \omega &= A^2 \sinh 2z \cos 2\alpha/2. \end{aligned}$$

The breather (5) is characterised by four real parameters: r, α, x_0, θ and one additional parameter θ_c . Parameters r and α are responsible for the breather shape, group velocity $V_{gr} = \gamma/\varkappa$ and phase velocity $V_{ph} = \omega/\eta$, while x_0 and θ describe breather position in space and its complex internal phase. The parameter θ_c is nothing more than the general phase of the condensate and usually is taken to be zero. However, in this work it plays the important role in the description of breathers interactions – see the text below. The mentioned Peregrine, Kuznetsov-Ma and Akhmediev breathers are the particular cases of the general solution (5) at $r = 1, \alpha = 0$; $r > 1, \alpha = 0$; and $r = 1, \alpha \neq 0$ correspondingly. The dynamics of these breathers is known well – see, for instance the paper [19]. Here we note, that Akhmediev breather describe periodic condensate perturbations while Peregrine and Kuznetsov-Ma breathers are the standing oscillating objects localised in space. The period of oscillations for Kuznetsov-Ma breather is defined by $1/\sinh 2z$ and tends to infinity when this solution transforms to the Peregrine breather in the limiting case $r \rightarrow 1$.

The condensate phase at infinity should be constant with time for any localized perturbations. Thus, the breather solutions capable to describe the growth of SLCP should have equal condensate phases at $x \rightarrow \pm\infty$, or at least have difference in the phases comparing with the relative value of the initial perturbation. A single breather changes the phase of the condensate before and after itself on 4α , that can be seen considering asymptotics of the expression (5) at $x \rightarrow \pm\infty$ [19].

Among one-breather solutions of the NLSE, only Kuznetsov-Ma and Peregrine breathers have equal condensate phases at infinity ($\alpha = 0$). As we discussed in the

Introduction these solutions were already considered for description of MI development. For a couple of breathers, the total change of phase before and after them is zero when

$$\alpha_1 = -\alpha_2. \quad (6)$$

Here and below indexes are used to distinguish breathers. As was found in the work [18] at certain phase synchronisation (close to $\theta_1 + \theta_2 = \pi$) and when the breather eigenvalues located near the branchcut ($r - 1 \ll 1$), such two-breather solution generate SLCP at certain moment of time. In the general case SLCP can be formed by \tilde{N} pairs of breathers satisfying the condition $\alpha_{2,j-1} = -\alpha_{2,j}$; $j = 1, \dots, \tilde{N}$. Such special type of exact solutions was called \tilde{N} -pair superregular breathers. The development of MI for the simplest one-pair symmetric superregular breather with parameters

$$\alpha_1 = -\alpha_2 = \alpha; \quad r_1 = r_2 = r; \quad r - 1 = \varepsilon \ll 1, \quad (7)$$

is presented in Fig. 1. Here $\varepsilon = r - 1$ plays the role of a small parameter characterising amplitude of the initial condensate perturbation. The initial (linear) stage of perturbation growth in this case is described by the following expression obtained in [19]:

$$\delta\psi \approx i\varepsilon A \frac{\cosh(i\alpha - 2\gamma t) \cos(2\eta x - (\theta_1 - \theta_2)/2)}{\cosh((2A\varepsilon \cos \alpha)x)}. \quad (8)$$

Here $\delta\psi$ is the SLCP: $\psi = A + \delta\psi$. The maximum value of the growth rate (defined by 2γ) for the expression (8) is achieved at $\alpha = \pi/4$. We can assume, that in this case superregular breather corresponds to the maximum of the MI growth rate (2), similar to the Akhmediev breather (see, for instance [23]). Indeed, when $\alpha = \pi/4$ ($Re[\lambda] = 1/\sqrt{2}$), maximum of the most significant Fourier spectrum sideband modes located at $k_{max} = \pm\sqrt{2}$ (with accuracy $\sim \varepsilon$) – see the Fig. 1.

It is important to discuss how the simple relation (6) looks in the λ parametrization (at least to compare theoretical predictions with recently published results [24–26], where the conventional spectral parameter is used). Obviously (6) defines the following family of parametric curves where the eigenvalues should be located:

$$\lambda_{Re} = \frac{A \cos \alpha}{2} \left(r + \frac{1}{r} \right), \quad \lambda_{Im} = \pm \frac{A \sin \alpha}{2} \left(r - \frac{1}{r} \right). \quad (9)$$

Here $\lambda_{Re, Im}$ are the real and imaginary parts of λ . The signs \pm correspond to the first and second breather in the pair. In the rest of the paper we will use the λ parametrization of spectral parameter and choose $A = 1$. The relationship between eigenvalue portraits on the conventional λ and uniformized ξ spectral planes can be easily understood from (4) and (9). For example, eigenvalues of Kuznetsov-Ma breather on the λ plane similarly located on the real axes after the branchcut: $Re[\lambda] > A$. For superregular eigenvalues we present typical parametric curves (9) in Fig. 2. According to the double sign

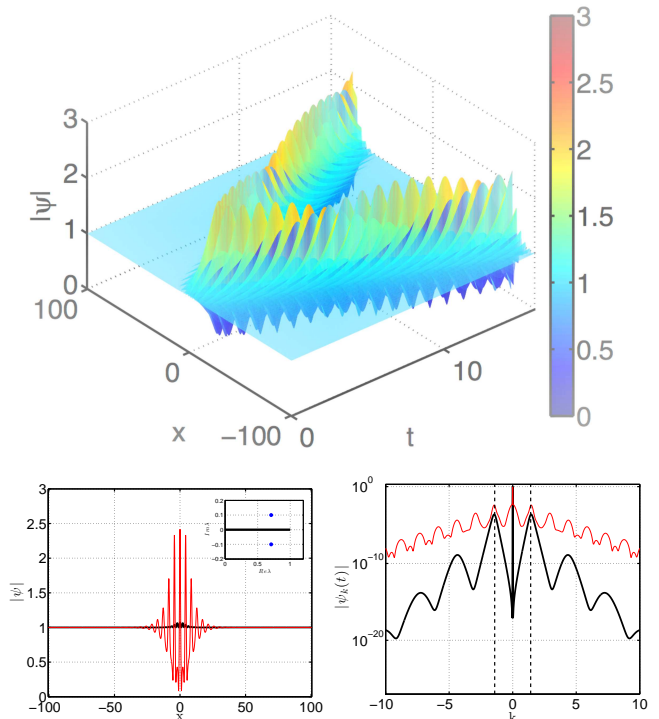


FIG. 1: Perturbation development driven by simplest superregular breather solution. Top picture demonstrates the whole space-time evolution of the wave field. Left and right pictures: amplitude profile and Fourier spectrum of the solution at the initial moment of time $t = 0$ (black bold lines) and at an intermediate stage of MI development ($t = 2$, red thin line). Black dotted lines corresponds to the value of k_{max} . Eigenvalues of breathers are shown on λ -plane – see the inset picture.

in (9) the eigenvalues of the first and second breather are located on opposite sides of the real axis. The SLCP are formed only by eigenvalues located on the grey (long dashed) and orange (short dashed) lines since the distance between the eigenvalues and the branchcut defines the amplitude of the initial perturbation.

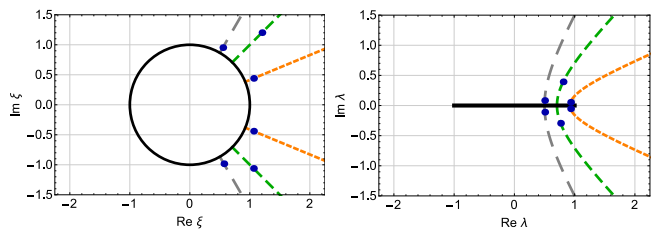


FIG. 2: Comparison of ξ and λ parametrizations of spectral parameter. The branch cut and its Joukowski mapping (4) are drawn by black solid lines. The pairs of breather eigenvalues (marked by blue points) lie on the rays (6) (dashed lines, left picture) and on the parametric curves (9) (dashed lines, right picture).

C. Breather interactions: space-phase shifts

To analyse multi-breather interactions we need exact expressions describing space-phase shifts that breathers acquire after collisions with each other. For soliton interactions on zero background such formulas are known since the paper of V.E. Zakharov and A.B. Shabat [6]. However, in the works devoted to the IST of the NLSE on the condensate background [7–9], the derivation of the breather space-phase shifts was skipped. To the best of our knowledge, these expressions have not been presented so far.

The general N -breather solution of the NLSE ψ_N can be written in the following form [18, 19]:

$$\psi_N = A + 2 \frac{\det \widetilde{M}_{1,2}}{\det M}, \quad \text{where } M_{nm} = \frac{(\mathbf{q}_n \cdot \mathbf{q}_m^*)}{\lambda_n + \lambda_m^*}, \quad (10)$$

$$\text{and } \widetilde{M}_{\alpha,\beta} = \begin{pmatrix} 0 & q_{1,\beta} & \cdots & q_{n,\beta} \\ q_{1,\alpha}^* & & & \\ \vdots & & M_{nm}^T & \\ q_{n,\alpha}^* & & & \end{pmatrix}.$$

Here, the two-component vectors $\mathbf{q}_n = (q_{n,1}, q_{n,2})$ are given by:

$$q_{n,1} = e^{-\phi_n} - \frac{iAe^{\phi_n}}{\lambda_n + \zeta_n}, \quad q_{n,2} = -\frac{iAe^{-\phi_n}}{\lambda_n + \zeta_n} + e^{\phi_n}, \quad (11)$$

the phase ϕ_n is

$$\phi_n = \zeta_n x - \text{Re}[\zeta_n]x_0 - i\lambda_n \zeta_n t - i\theta_n/2, \quad (12)$$

and the function $\zeta_n = \sqrt{A^2 - \lambda_n^2}$ defines the branchcut of the spectral parameter plane.

We solve space-phase shifts problem using standard technique: asymptotic analysis of two-breather solution, that can be obtained from (10) at $N = 2$. Considering asymptotic states of separate breathers at $t \rightarrow \pm\infty$ we find the following expressions, that describe space shift $\Delta x_{0,2}$ and phase shifts $\Delta\theta_2, \Delta\theta_{c,2}$ that the breather 2 acquires after collision with the breather 1:

$$\Delta x_{0,21} = \frac{1}{2\text{Re}[\zeta_2]} \ln \left(\frac{s_1 - s_3}{s_2 - s_4} \right), \quad (13)$$

$$\Delta\theta_{21} = 2\text{Arg}[i^2(p_1 - p_2)]; \quad \Delta\theta_{c,21} = -4\text{Arg}[i(\lambda_1 + \zeta_1)],$$

where

$$\begin{aligned} s_1 &= (A^4 + |\lambda_1 + \zeta_1|^2 \cdot |\lambda_2 + \zeta_2|^2) \cdot |\lambda_1 + \lambda_2^*|^2 + \\ &\quad + A^2(|\lambda_1 + \zeta_1|^2 + |\lambda_2 + \zeta_2|^2) \cdot |\lambda_1 - \lambda_2|^2, \\ s_2 &= A^2(|\lambda_1 + \zeta_1|^2 + |\lambda_2 + \zeta_2|^2) \cdot |\lambda_1 + \lambda_2^*|^2 + \\ &\quad + (A^4 + |\lambda_1 + \zeta_1|^2 \cdot |\lambda_2 + \zeta_2|^2) \cdot |\lambda_1 - \lambda_2|^2, \\ s_3 &= A^2(\lambda_1 + \lambda_1^*)(\lambda_2 + \lambda_2^*) \cdot [(\lambda_1 + \zeta_1)(\lambda_2 + \zeta_2) + \\ &\quad + (\lambda_1^* + \zeta_1^*)(\lambda_2^* + \zeta_2^*)], \\ s_4 &= A^2(\lambda_1 + \lambda_1^*)(\lambda_2 + \lambda_2^*) \cdot [(\lambda_1 + \zeta_1)(\lambda_2^* + \zeta_2^*) + \\ &\quad + (\lambda_1^* + \zeta_1^*)(\lambda_2 + \zeta_2)]; \\ p_1 &= \{A^2(\lambda_2 + \zeta_2 + \lambda_1^* + \zeta_1^*) + |\lambda_1 + \zeta_1|^2(\lambda_2^* + \zeta_2^*) + \\ &\quad + |\lambda_2 + \zeta_2|^2(\lambda_1 + \zeta_1)\} / \{|\lambda_1 + \lambda_2^*|^2\}, \\ p_2 &= \frac{(A^2 + |\lambda_1 + \zeta_1|^2)(\lambda_2 + \zeta_2 + \lambda_2^* + \zeta_2^*)}{(\lambda_1 + \lambda_1^*)(\lambda_2 + \lambda_2^*)}. \end{aligned}$$

Here we use additional general phase θ_c (defined in (5)) for the second breather to describe how the first breather reverse condensate phase after itself. One can check, that at $A \rightarrow 0$ expressions (13) become well-known soliton space-phase shifts, so that the two phases θ_2 and $\theta_{c,2}$ form a single soliton phase.

D. Rogue waves formation as a result of superregular breathers collisions

It is well known, that collisions of the NLSE breathers with particular phases can produce typical rogue waves [2, 27, 28]. The formation of SLCP by superregular solutions is the back side of this process. Indeed, depending on the sum of the breathers phases: $\theta_1 + \theta_2$, amplitude profile at the moment of collision can vary from a small perturbation to the rogue wave of extreme amplitude, that we discussed in the paper [20] and here illustrate by Fig. 3.

Nevertheless, scenario when the moving NLSE breathers appear from SLCP and then produce the rogue waves by collisions with each other has not been studied so far. We found, that pairs of superregular breathers being synchronised inside each pair can be additionally synchronised between each other to produce the rogue wave at the nonlinear stage of the MI development. Such two-step synchronisation demands to account space-phase shifts (13), that we can perform analytically – see details in the Appendix section. This new scenario of rogue waves formation for the simplest four-breather model with symmetric eigenvalues is presented in Fig. 4. Perturbations generate four breathers as a result of MI, then two of them moving towards each other collide and produce the rogue wave.

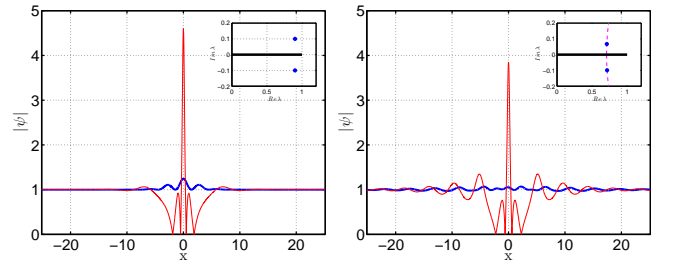


FIG. 3: Amplitude profiles of two-breather collision. Blue bold lines correspond to superregular synchronisation ($\theta_1 + \theta_2 = \pi$), while red thin lines show the rogue wave formation at $\theta_1 + \theta_2 = 2\pi$. The inset pictures demonstrate breather eigenvalues. Left and right pictures correspond to symmetric and nonsymmetric breathers. The dashed magenta line shows that discrete eigenvalues in nonsymmetric case lie on the parametric curves (9).

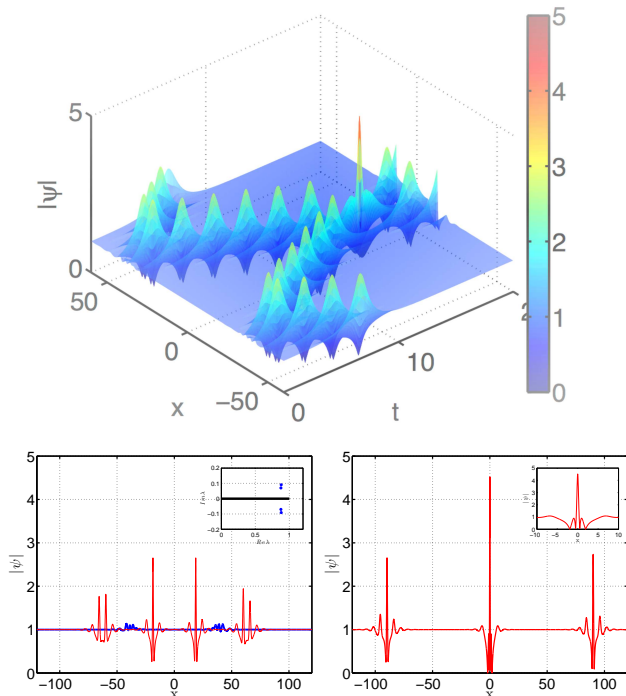


FIG. 4: New scenario of rogue waves formation from the locally perturbed condensate. Top picture demonstrates the whole space-time evolution of the wave field. Left picture represents the initial condensate perturbations – two pairs of superregular breathers (blue solid line); the intermediate stage at $t = 7$ (thin red lines) and breathers eigenvalues (inset picture). Right picture demonstrates the moment of rogue wave formation at $t = 15$.

E. Rogue wave formation from the randomly perturbed condensate

The suggested scenario of rogue waves formation can be observed not only for the manually synchronised breathers, but also for the random distribution of superregular condensate perturbations. In Fig. 5 we present the example of 16-breather MI development. At the initial moment of time, the condensate is locally perturbed by randomly distributed in space 8 superregular pairs – see the left picture. In this case the breather phases in each pair can be synchronised separately, so we can generate initial condition without using formulas (13). On the right picture we show the most significant rogue wave observation over 100 random initial condition runs. Note, that simulation of multi-breather solution by exact formulas is the ill-conditioned problem at large number of breathers (we recently discuss the same problem for solitons in [29] and [30]). Here we use Zakharov-Shabat dressing method (alternative formulation of the N -breather solution (10) – see our previous works [18, 19] for details) supplemented by arbitrary precession arithmetics to mitigate numerical instability and generate accurate 8-pair superregular initial conditions.

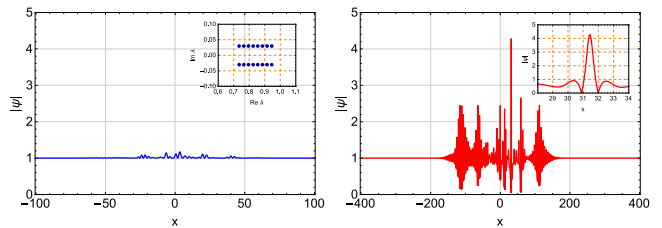


FIG. 5: Rogue waves formation from the condensate locally perturbed by randomly distributed 8 pairs of superregular breathers. Left picture shows the initial condition at $t = 0$, while the moment of maximum amplitude generation ($t_{max} = 9.042$) is presented on the right. The inset pictures demonstrate breather eigenvalues and magnification of the generated rogue wave.

The final question is of key importance – do superregular breathers are contained in arbitrary type SLCP? Indeed, the ability of superregular breathers to produce the broad family of initial conditions was demonstrated many times [18–20], but the inverse task – decomposition of arbitrary initial condensate perturbation into elementary nonlinear modes including superregular breathers have not been considered so far. Here we study spectrum of ZH system (3) for several general types of randomly generated SLCP and demonstrate that superregular pairs of eigenvalues are presented in the spectrum.

We use M harmonics with arbitrary phases, belonging unstable part of the MI growth rate (2) and modulate them by different functions $f(x, \sigma)$ to obtain localised perturbation (σ is the spatial width of the perturbation):

$$\delta\psi(x) = \epsilon\rho f(x, \sigma) \sum_{j=1}^M \sin(k_j x + \varphi_j), \quad (14)$$

$$k_j = k_0 + \Delta k(j - 1 - M/2); \quad \varphi_j \in [0, 2\pi].$$

Here $\rho = 1$ or i , while ϵ characterises the perturbation amplitude. We use several harmonics ($M \sim 10$) and vary modulation functions. Then we solve ZH eigenvalue problem using standard Fourier collocation method [31] with high numerical accuracy. We study initial perturbation at large numerical interval equal to $1024 \cdot \pi$ and use 16384 discretisation points (the latter corresponds to the maximum performance of 192GB RAM). This allows us to avoid the effect of periodicity (which is manifested by the appearance of finite-gap zones in the eigenvalue spectrum – see the recent preprint [32], where such finite gap spectrum was described) and unambiguously identify discrete spectrum eigenvalues.

Symmetric superregular breathers (7) at $\theta_1 = \theta_2 = \pi/2$ and arbitrary (even not necessary small) value of ϵ , generate pure imaginary condensate perturbation (remember, we assume that condensate is the real constant). This can be exactly proved considering two-breather solution at $t = 0$ and approximately (with accuracy $\sim \epsilon^2$) is seen from the expression (8). Thus, first of all, we study pure imaginary condensate perturbations, i.e. the case $\rho = i$

in (14). For several random runs with modulation functions $f = \text{sech}(\sigma x)$ and $f = \exp(-x^2/\sigma^2)$ we clearly observe different distributions of symmetric eigenvalues near the branchcut – the example is presented in Fig. 6 (left). In addition we studied pure real perturbations. In this case we find eigenvalues on the real axes very close to the branch point – see Fig. 6 (right). The latter corresponds to the scenario with "almost" Peregrine breathers suggested by V.I. Shrira and V.V. Geogjaev [17] (see the *Introduction*).

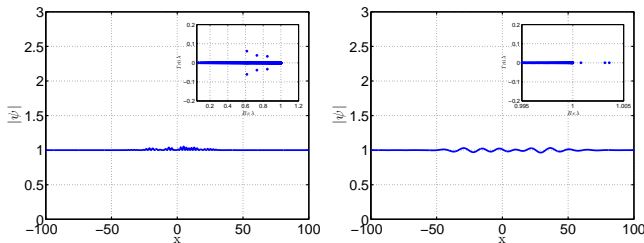


FIG. 6: Eigenvalues of arbitrary-type SLCP. Left: imaginary perturbation generated via (14) with $M = 8$, $k_0 = \sqrt{2}$, $dk = 0.1$ and $f(x) = \exp(-x^2/30^2)$ and $\epsilon = 10^{-1}$. Right: real perturbation generated in similar way with $M = 8$, $k_0 = 0.4$, $dk = 0.025$; $f(x) = \exp(-x^2/40^2)$ and $\epsilon = 2 \cdot 10^{-2}$.

F. Discussion and Conclusion

In this paper we demonstrate that superregular breathers are the important part of scattering data for arbitrary-type condensate perturbations and play the key role in the formation of rogue waves as a result of MI. We show, that pure imaginary perturbations contain symmetric superregular breathers, while pure real perturbations contain Kuznetsov-Ma breathers with eigenvalues close to the branch point (almost Peregrine solution). However, the eigenvalue spectrum of arbitrary-type perturbations does not reveal the impact of the continuous spectrum waves. The numerical simulation of the evolution of the perturbations presented in Fig. 6 shows complicated wave patterns which, apparently, are driven by nonlinear interaction of breathers and continuous spectrum (stable and unstable parts) waves. This question demands a separate study.

We show, that the eigenvalue spectrum is the powerful tool to analyse the nonlinear nature of the arbitrary-type condensate perturbations. The next step is to consider combinations of imaginary and real perturbations or perturbations based on the broadband random noise. For the latter case, B. Kibler et al. found strong signatures of superregular breathers at the intermediate stage of the MI development [33].

The other question is the study of MI development from spatially periodic perturbations, that is highly important to explain some results of recent statistical numerical experiments of D.S. Agafontsev and V.E. Za-

kharov with the NLSE on unstable backgrounds [34, 35]. The significant progress in this field was made recently by J.M. Soto-Crespo, N. Devine and N. Akhmediev, who attributed the formation of rogue waves from the stochastic periodic condensate perturbations to the breather collisions [24, 25] and S. Randoux, P. Suret and G. El, who links this phenomena with the so called *multi-phase (finite-band)* solutions of the NLSE [26]. We believe, that superregular breathers also can appear in such numerical simulations when the size of the numerical tank is significantly larger than typical width of superregular perturbations, that can be estimated as $1/(\epsilon \cos \alpha)$ in accordance with (8).

In this work we also discuss the relationship between eigenvalue portraits on the conventional λ and uniformized ξ spectral planes, that is intended to link several works in this field. Finally we note, that found in this paper space-phase shifts describing NLSE breathers collisions can be used for different further studies. Among them, experimental realisation of complicated multi-breather dynamics is of special interest.

G. Acknowledgments

The author is thankful to 1) Prof. V.E. Zakharov for providing the idea to study imaginary and real condensate perturbations separately; 2) Prof. E.A. Kuznetsov for the helpful discussions of the continuous spectrum waves; 3) Dr. D.S. Agafontsev for the helpful comments with regard to Fourier spectrum of superregular breathers and discussion of possible applications of the presented results in the interpretation of numerical simulations with periodically perturbed condensate; 4) Dr. B. Kibler for the helpful discussions of the broadband random noise SLCP. Numerical code and simulations were performed at the Novosibirsk Supercomputer Center (NSU). The work was performed by supporting of the Russian Science Foundation (Grand No. 14-22-00174).

H. Appendix: details of breather collisions synchronization

Now we discuss synchronization of four-breather MI development presented in Fig. 4. We choose the initial moment of time as $t_0 = 0$ and the moment when we expect to observe the rogue wave formation (maximum of its amplitude) as $t_{max} = 15$ at $x = 0$. The problem is to find initial space shifts and phases for each of four breathers. Let us denote breathers in the left superregular pair by indexes 1 (the breather moving to the left) and 2 (the breather moving to the right) and breathers in the second pair by indexes 3 (the breather moving to the left) and 4 (the breather moving to the right). The breathers 2 and 3 have complex conjugated eigenvalues, so they differ only in the direction of the group velocity: $V_{gr2} = -V_{gr3} = \tilde{V}_{gr}$. Before the moment $t = 0$, the

breather 2 was affected by collisions with the breathers 1 and 4, so the total space shift for it should be written as:

$$x_{0,2} = -\tilde{V}_{gr} \cdot t_{max} - \Delta x_{0,12} + \Delta x_{0,42}. \quad (15)$$

To obtain further synchronization inside the left superregular pair, we should choose the same space shift for the breather 1 as well: $x_{0,1} = x_{0,2}$. By analogy we obtain the following space shifts for the breathers 3 and 4:

$$x_{0,3} = x_{0,4} = \tilde{V}_{gr} \cdot t_{max} - \Delta x_{0,13} + \Delta x_{0,43}. \quad (16)$$

Synchronization of phases we start again from the breathers 2 and 3. According to the Fig. 3 the phases of both breathers should be equal π , but we have to account the phase changing with time t_{max} and phase shifts acquired after collisions with breathers 1 and 4. Denoting the phase velocity for the second and third breather

as $V_{ph_2} = V_{ph_3} = \tilde{V}_{ph}$ we obtain:

$$\theta_2 = \theta_3 = \pi + \tilde{V}_{ph} \cdot t_{max} - \Delta\theta_{12} + \Delta\theta_{42}. \quad (17)$$

Now the formation of the rogue wave at t_{max} , $x = 0$ is obtained and we only need to synchronise formation of small condensate superregular perturbations at $t = 0$. As we discussed in the main text of the paper superregular synchronization appear at $\theta_1 + \theta_2 = \pi$ (see again the Fig. 3). The breather 1 was affected by collisions with the breathers 3 and 4, while the breather 4 collided with breathers 3 and 1. Thus, the required phase shifts can be found as:

$$\begin{aligned} \theta_1 &= \pi - \theta_2 - \Delta\theta_{13} - \Delta\theta_{14}, \\ \theta_4 &= \pi - \theta_3 + \Delta\theta_{43} - \Delta\theta_{14}. \end{aligned} \quad (18)$$

-
- [1] V. E. Zakharov and L. A. Ostrovsky, *Physica D: Nonlinear Phenomena* **238**, 540 (2009).
- [2] C. Kharif, E. Pelinovsky, and A. Slunyaev, *Rogue waves in the ocean, observation, theories and modeling* (Advances in Geophysical and Environmental Mechanics and Mathematics Series, Springer, Heidelberg, 2009).
- [3] D. R. Solli, C. Ropers, P. Koonath, and B. Jalali, *Nature* **450**, 1054 (2007).
- [4] V. B. Efimov, A. N. Ganshin, G. V. Kolmakov, P. V. E. McClintock, and L. P. Mezhev-Deglin, *Eur. Phys. J. Special Topics* **185**, 181 (2010).
- [5] A. Chabchoub, N. P. Hoffmann, and N. Akhmediev, *Physical Review Letters* **106**, 204502 (2011).
- [6] V. E. Zakharov and A. B. Shabat, *Soviet Physics JETP* **34**, 62 (1972).
- [7] E. A. Kuznetsov, in *Akademiia Nauk SSSR. Doklady*, Vol. 236 (1977) pp. 575–577.
- [8] Y.-C. Ma, *Studies in Applied Mathematics* **60**, 43 (1979).
- [9] T. Kawata and H. Inoue, *Journal of the Physical Society of Japan* **44**, 1968 (1978).
- [10] D. H. Peregrine, *J. Austral. Math. Soc. Ser. B. Appl. Math.* **25**, 16 (1983).
- [11] N. N. Akhmediev, V. M. Eleonskii, and N. E. Kulagin, *Sov. Phys. JETP* **62**, 894 (1985).
- [12] E. Kuznetsov, *JETP letters* **105**, 108 (2017).
- [13] G. Biondini and D. Mantzavinos, *Physical Review Letters* **116**, 043902 (2016).
- [14] G. Biondini, S. Li, and D. Mantzavinos, *Physical Review E* **94**, 060201 (2016).
- [15] N. Akhmediev, A. Ankiewicz, and J. M. Soto-Crespo, *Phys. Rev. E* **80**, 026601 (2009).
- [16] P. Dubard and V. B. Matveev, *Nonlinearity* **26**, R93 (2013).
- [17] V. I. Shrira and V. V. Geogjaev, *J. Eng. Math.* **67**, 11 (2010).
- [18] V. E. Zakharov and A. A. Gelash, *Physical Review Letters* **111**, 054101 (2013).
- [19] A. A. Gelash and V. E. Zakharov, *Nonlinearity* **27**, R1 (2014).
- [20] B. Kibler, A. Chabchoub, A. Gelash, N. Akhmediev, and V. E. Zakharov, *Phys. Rev. X* **5**, 041026 (2015).
- [21] J.-H. Zhang, L. Wang, and C. Liu, in *Proc. R. Soc. A*, Vol. 473 (The Royal Society, 2017) p. 20160681.
- [22] C. Liu, Y. Ren, Z.-Y. Yang, and W.-L. Yang, *Chaos: An Interdisciplinary Journal of Nonlinear Science* **27**, 083120 (2017).
- [23] N. Akhmediev, A. Ankiewicz, J. M. Soto-Crespo, and J. M. Dudley, *Phys. Lett. A* **375**, 775 (2011).
- [24] J. M. Soto-Crespo, N. Devine, and N. Akhmediev, *Physical Review Letters* **116**, 103901 (2016).
- [25] N. Akhmediev, J. M. Soto-Crespo, and N. Devine, *Physical Review E* **94**, 022212 (2016).
- [26] S. Randoux, P. Suret, and G. El, *Scientific reports* **6** (2016).
- [27] N. Akhmediev, J. M. Soto-Crespo, and A. Ankiewicz, *Phys. Rev. A* **80**, 043818 (2009).
- [28] N. Akhmediev, J. M. Soto-Crespo, and A. Ankiewicz, *Phys. Lett. A* **373**, 2137 (2009).
- [29] A. Gelash and D. Agafontsev, in *Proceedings of EGU-General Assembly, Vienna, Austria*, Vol. 19 (2017) p. 15446.
- [30] L. Frumin, A. Gelash, and S. Turitsyn, *Physical Review Letters* **118**, 223901 (2017).
- [31] Y. Jianke, *Nonlinear waves in integrable and nonintegrable systems*, Vol. 16 (Society for Industrial and applied Mathematics, Philadelphia, 2010).
- [32] P. Grinevich and P. Santini, arXiv preprint arXiv:1707.05659 (2017).
- [33] B. Kibler, A. Chabchoub, A. Gelash, N. Akhmediev, and V. E. Zakharov, *Nonlinear Guided Wave Optics: A testbed for extreme waves* (IOP Publishing Ltd, Editor: Stefan Wabnitz, to be published).
- [34] D. S. Agafontsev and V. E. Zakharov, *Nonlinearity* **28**, 2791 (2015).
- [35] D. S. Agafontsev and V. E. Zakharov, *Nonlinearity* **29**, 3551 (2016).